

# PARAMETRIC ANALYSES OF AN ABSORPTION REFRIGERATION SYSTEM WITH WATER AND LITHIUM BROMIDE IN STEADY STATE POWERED BY SOLAR ENERGY

V. Prendin<sup>a</sup>,L. C. Martinez<sup>b</sup>and N. M. S. Kaminari<sup>c</sup>

<sup>a</sup>Pontificia Universidade Católica do Paraná  
Departamento de Engenharia Mecânica  
Bairro Prado Velho  
CEP. 80215-901, Curitiba, Paraná, Brasil  
prendinvitor@gmail.com

<sup>b</sup>Pontificia Universidade Católica do Paraná  
Departamento de Engenharia Mecânica  
Bairro Prado Velho  
CEP. 80215-901, Curitiba, Paraná, Brasil  
leonardo.cavalheiro@pucpr.br

<sup>c</sup>Pontificia Universidade Católica do Paraná  
Departamento de Engenharia Mecânica  
Bairro Prado Velho  
CEP. 80215-901, Curitiba, Paraná, Brasil  
nice.kaminari@pucpr.br

Received: Mar 07, 2022

Revised: Mar 25, 2022

Accepted: Mar 26, 2022

## ABSTRACT

The demand of energy utilization is increasing expressively as fast as the development of countries. Besides being available everywhere and virtual inexhaustible, renewable energy is undoubtedly necessary to avoid depleting the planet's natural resources and global warming. Even considering the primordial environmental importance, the result of no emissions by renewable energy grant attractive also for political and economics statement. It should be noted the sun is the most abundant primary energy source in the planet and essential for eco-friendly process like photosynthesis, wind action, water cycle as well direct uses as electric and thermal generations. Consequently, nowadays several methodologies have been applied in order to transfer energy between the cycle and its surroundings optimizing for instance the coefficient of performance and heat exchangers. An absorption system is widely applied in these cases due to supply a unique solution for a range of technological problems from solar cooling to steam-driven refrigeration. Alternatively, this article main objective is modulating an absorption refrigeration system (ARS) which uses water-lithium bromide as a working fluid. Therefore, using the software Engineering Equation Solver (EES) is possible to obtain a thermodynamic single effect code that allows elaborating parametric analyses. In other words, performed and verified the influence of some input parameters over other output parameters. First, it was necessary to consider the cycle operating as reversible and steady state. Furthermore, it is assumed that no chemical reactions occur between water and lithium bromide. Thus, in the meantime apply the heat exchangers and a Solar Collector to receive the thermal energy and provide to the refrigeration cycle. Similarly, water from external sources was used to change heat with the fluid water-lithium bromide. Satisfactory results were founded and it enable to calculate and evaluate all system heat transfers rates and coefficient of performance. Almost all of input parameters introduced brought adequate values over output parameters, but the most convenient were: mass balance of water-lithium bromide solution and temperature of cold water from outside source. Clearly, results always can be found but in conclusion this article can be used to verify parameters sensitivity, optimized absorption refrigeration solutions and supply knowledge for future applications.

**Keywords:** renewable energy, absorption refrigeration systems, engineering equation solver, refrigeration cycle, water-lithium bromide

## NOMENCLATURE

$A_{cs}$	solar collectors' area, m <sup>2</sup>	$h_4$	enthalpy flow of refrigerant fluid in the exit of the Thermal Generator and in the entrance of the Heat Exchanger, kg/s
$C_p$	water specific heat, J/kg°C	$h_5$	enthalpy flow of refrigerant fluid in the exit of the Thermal Generator and in the entrance of the Expansion Valve, kg/s
COP	coefficient of performance, %	$h_6$	enthalpy flow of refrigerant fluid in the exit of the Expansion Valve and in the entrance of the Absorber, kg/s
$E_{cs}$	useful energy, kWh	$h_7$	enthalpy flow of refrigerant fluid in the exit of the Thermal Generator and in the entrance of the Condenser, kg/s
$h_1$	enthalpy flow of refrigerant fluid in the exit of the Absorber and in the entrance of the Pump, kg/s	$h_8$	enthalpy flow of refrigerant fluid in the exit of the Condenser and in the entrance of the Expansion Valve, kg/s
$h_2$	enthalpy flow of refrigerant fluid in the exit of the Pump and in the entrance of the Heat Exchanger, kg/s		
$h_3$	enthalpy flow of refrigerant fluid in the exit of the Heat Exchanger and in the entrance of the Thermal Generator, kg/s		

$h_9$	enthalpy flow of refrigerant fluid in the exit of the Expansion Valve and in the entrance of the Evaporator, kg/s	$\dot{m}_{11}$	mass flow in the entrance of hot water from the Solar Collector, kg/s
$h_{10}$	enthalpy flow of refrigerant fluid in the exit of the Evaporator and in the entrance of the Absorber, kg/s	$\dot{m}_{12}$	mass flow in the exit of hot water from the Solar Collector, kg/s
$h_{11}$	enthalpy flow in the entrance of hot water from the Solar Collector, kg/s	$\dot{m}_{13}$	mass flow in the entrance of condensation water from the external source, kg/s
$h_{12}$	enthalpy flow in the exit of hot water from the Solar Collector, kg/s	$\dot{m}_{14}$	mass flow in the entrance of condensation water from the external source, kg/s
$h_{13}$	enthalpy flow in the entrance of condensation water from the external source, kg/s	$\dot{m}_{15}$	mass flow of refrigerant fluid in the entrance of condensation water from the external source, kg/s
$h_{14}$	enthalpy flow in the entrance of condensation water from the external source, kg/s	$\dot{m}_{16}$	mass flow of refrigerant fluid in the exit of condensation water from the external source, kg/s
$h_{15}$	enthalpy flow of refrigerant fluid in the entrance of condensation water from the external source, kg/s	$\dot{m}_{17}$	mass flow of refrigerant fluid in the entrance of cold water from the external source, kg/s
$h_{16}$	enthalpy flow of refrigerant fluid in the exit of condensation water from the external source, kg/s	$\dot{m}_{18}$	mass flow of refrigerant fluid in the exit of cold water from the external source, kg/s
$h_{17}$	enthalpy flow of refrigerant fluid in the entrance of cold water from the external source, kg/s	$\dot{Q}_a$	heat transfer rate rejected by the Absorber, kW
$h_{18}$	enthalpy flow of refrigerant fluid in the exit of cold water from the external source, kg/s	$\dot{Q}_c$	heat transfer rate rejected by the Condenser, kW
$I$	average of solar normal irradiations in Brasilia, kWh/m <sup>2</sup> day	$\dot{Q}_e$	heat transfer rate absorbed by the Evaporator, kW
$K$	Solar Collector efficiency, %	$\dot{Q}_g$	heat transfer rate absorbed by the Thermal Generator, kW
$\dot{m}_1$	mass flow of refrigerant fluid in the exit of the Absorber and in the entrance of the Pump, kg/s	$\dot{Q}_{tc}$	heat transfer rate that occurs between the hot and the cold side of the Heat Exchanger, kW
$\dot{m}_2$	mass flow of refrigerant fluid in the exit of the Pump and in the entrance of the Heat Exchanger, kg/s	$T_1$	temperature of refrigerant fluid in the exit of the Absorber and in the entrance of the Pump, °C
$\dot{m}_3$	mass flow of refrigerant fluid in the exit of the Heat Exchanger and in the entrance of the Thermal Generator, kg/s	$T_2$	temperature of refrigerant fluid in the exit of the Pump and in the entrance of the Heat Exchanger, °C
$\dot{m}_4$	mass flow of refrigerant fluid in the exit of the Thermal Generator and in the entrance of the Heat Exchanger, kg/s	$T_3$	temperature of refrigerant fluid in the exit of the Heat Exchanger and in the entrance of the Thermal Generator, °C
$\dot{m}_5$	mass flow of refrigerant fluid in the exit of the Thermal Generator and in the entrance of the Expansion Valve, kg/s	$T_4$	temperature of refrigerant fluid in the exit of the Thermal Generator and in the entrance of the Heat Exchanger, °C
$\dot{m}_6$	mass flow of refrigerant fluid in the exit of the Expansion Valve and in the entrance of the Absorber, kg/s	$T_5$	temperature of refrigerant fluid in the exit of the Thermal Generator and in the entrance of the Expansion Valve, °C
$\dot{m}_7$	mass flow of refrigerant fluid in the exit of the Thermal Generator and in the entrance of the Condenser, kg/s	$T_6$	temperature of refrigerant fluid in the exit of the Expansion Valve and in the entrance of the Absorber, °C
$\dot{m}_8$	mass flow of refrigerant fluid in the exit of the Condenser and in the entrance of the Expansion Valve, kg/s	$T_7$	temperature of refrigerant fluid in the exit of the Thermal Generator and in the entrance of the Condenser, °C
$\dot{m}_9$	mass flow of refrigerant fluid in the exit of the Expansion Valve and in the entrance of the Evaporator, kg/s	$T_8$	temperature of refrigerant fluid in the exit of the Condenser and in the entrance of the Expansion Valve, °C
$\dot{m}_{10}$	mass flow of refrigerant fluid in the exit of the Evaporator and in the entrance of the Absorber, kg/s	$T_9$	temperature of refrigerant fluid in the exit of the Expansion Valve and in the entrance of the Evaporator, °C
		$T_{10}$	temperature of refrigerant fluid in the exit of the Evaporator and in the entrance of the Absorber, °C

$T_{11}$	temperature in the entrance of hot water from the Solar Collector, °C
$T_{12}$	temperature in the exit of hot water from the Solar Collector, °C
$T_{13}$	temperature in the entrance of condensation water from the external source, °C
$T_{14}$	temperature in the entrance of condensation water from the external source, °C
$T_{15}$	temperature of refrigerant in the entrance of condensation water from the external source, °C
$T_{16}$	temperature of refrigerant in the exit of condensation water from the external source, °C
$T_{17}$	temperature of refrigerant fluid in the entrance of cold water from the external source, °C
$T_{18}$	temperature of refrigerant fluid in the exit of cold water from the external source, °C
$T_{19}$	average temperature of Brasília, °C
$UA_a$	Absorber thermal conductance, kW/K
$UA_c$	Condenser thermal conductance, kW/K
$UA_e$	Evaporator thermal conductance, kW/K
$UA_g$	Thermal Generator thermal conductance, kW/K
$UA_{tc}$	Heat Exchanger thermal conductance, kW/K
$V$	water volume to be heated, m <sup>3</sup>
$\dot{W}_b$	Pump work in the control volume, kW
$x_1$	strong concentration of lithium bromide solution, %
$x_3$	concentration of lithium bromide solution, %
$x_4$	concentration of lithium bromide solution, %
$x_6$	weak concentration of lithium bromide solution, %

### Greek symbols

$\varepsilon_{tc}$	Heat Exchanger effectiveness, %
--------------------	---------------------------------

### Subscripts

a	Absorber
c	Condenser
e	Evaporator
g	Thermal Generator
lmtD	logarithmic mean temperature difference

## INTRODUCTION

Since the end of 18<sup>th</sup> century as a result of high demand of traditional energies, the increase of emission gases especially monoxide and dioxide carbon have been taking into account at international programs and scientific meetings. In consequence, renewable energy started being considered an alternative to replace traditional energies due the need to avoid depleting the planet's natural resources and global warming (Moreira, 2009).

Solar energy is an example of renewable energy that is currently highly used for electric and thermal generation. Additionally, it depends on high levels of local direct radiation. Hence, it is indispensable to evaluate this radiation and sunlight by using two technical instruments called pyranometers and

heliographs. The levels of solar radiation change accordingly to inclination of sun orbit rotation. Furthermore, also with year period, region and especially with some essential parameters such as altitude and meteorological conditions included humidity, concentration of emissions and cloudiness (Reis, 2019).

The Figure 1 reveals a map which indicates where the highest solar normal irradiances in Brazil are.

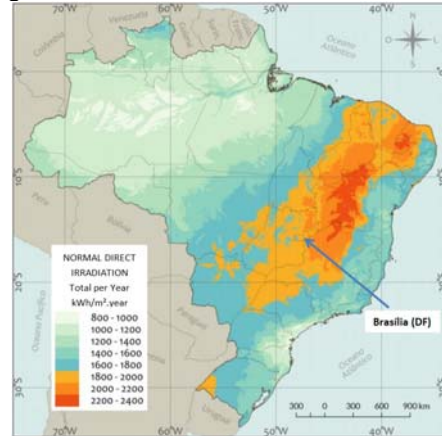


Figure 1. Solar normal irradiances in Brazil per Year (Pereira, 2017).

The development of this article considered the city of Brasília, located in Federal District of Brazil to install an absorption refrigeration system. With this in mind, the city conditions are given by a national organization of environment system that mention solar radiation of 5,38 kWh/m<sup>2</sup>.day, altitude of 1023 meters, latitude of -15.601 South, longitude of -47.713 West and tropical climate with an average temperature of 22 °C (Sonda, 2019).

An absorption refrigeration system powered by solar energy is widely applied in these cases due to its easy accessibility to reach temperatures from 100 to 270 and also the advantage of using heat sources for single-effect, double-effect or triple-effect systems. Technological problems as solar cooling and steam-driven refrigeration provide a unique solution for an absorption cycle since eliminate the need of a work input.

As revealed by Clausius statement of second law of thermodynamics, Heat Pump is a device responsible to transfer heat from a low temperature to a high temperature as evidence in refrigeration systems and heat pump heating systems. However, there are some strategies to provide the heat-pumping function by changing the type of energy input, whether heat or work. Absorption systems are an example of heat-driven technology that transfers energy between the cycle and its surroundings, besides are sorted according to a combination of three working fluids: water/lithium bromide chillers, ammonia/water chillers, and ammonia/water/hydrogen refrigerators (Herold, 2016).



$$\sum_e \dot{m}_e = \sum_s \dot{m}_s \quad (1.1)$$

$$\frac{dE_{vc}}{dt} = \dot{Q}_{vc} - \dot{W}_{vc} + \sum_e \dot{m}_e \left( h_e + \frac{V_e^2}{2} + g \cdot z_e \right) - \sum_s \dot{m}_s \left( h_s + \frac{V_s^2}{2} + g \cdot z_s \right) \quad (2)$$

$$\dot{Q}_{vc} = -\dot{W}_{vc} + \sum_s \dot{m}_s \left( h_s + \frac{V_s^2}{2} + g \cdot z_s \right) - \sum_e \dot{m}_e \left( h_e + \frac{V_e^2}{2} + g \cdot z_e \right) \quad (2.1)$$

$$\dot{Q}_{vc} = -\dot{W}_{vc} + \sum_s \dot{m}_s (h_s) - \sum_e \dot{m}_e (h_e) \quad (2.2)$$

where  $\frac{dm_{vc}}{dt}$ ,  $\sum_e \dot{m}_e$ ,  $\sum_s \dot{m}_s$  are the temporal rate of

mass variation in the control volume and the sum of input and output mass flow, respectively. Additionally,

$\frac{dE_{vc}}{dt}$ ,  $\dot{W}_{vc}$ ,  $h$ ,  $\frac{V^2}{2}$  and  $z$  are the temporal rate of

energy variation in the control volume, pump work, enthalpy flow, kinetic energy and gravitational potential, respectively. The kinetic and potential energy variations are neglected. Finally,

$\dot{Q}_{vc}$ ,  $\dot{W}_{vc}$  are the net heat transfer energy rate in the control volume and the net energy transfer rate per work in the control volume, respectively.

Below, the main equations for all components that guide the absorption refrigeration system are described separately.

### Evaporator

In the Evaporator, a heat exchange occurs between the refrigerant fluid and the cold water that is coming from the external source, Equations (3) e (4). Thus, heat is absorbed by the ARS and the mixture of liquid and water vapor are converted into saturated water vapor. Therefore, the energy balance in the Evaporator is given by Equation (5).

$$\dot{m}_9 = \dot{m}_{10} \quad (3)$$

$$\dot{m}_{17} = \dot{m}_{18} \quad (4)$$

$$\dot{Q}_e = \dot{m}_{10} h_{10} - \dot{m}_9 h_9 \quad (5)$$

where  $\dot{m}_9$ ,  $\dot{m}_{10}$ ,  $h_{10}$ ,  $h_9$  are the mass and enthalpy flow of refrigerant fluid in the entrance and exit of the Evaporator. On the other hands,  $\dot{m}_{17}$ ,  $\dot{m}_{18}$  are the mass

flow in the entrance and exit of cold water from the external source.

The heat transfer rate  $\dot{Q}_e$  occurs simultaneously between the Evaporator and the external source, Equation (6). Consequently, the logarithmic mean temperature difference (LMTD) method is used according to Equation (7) to modulate this component.

$$\dot{Q}_e = UA_e \Delta T_{lm,e} \quad (6)$$

$$\Delta T_{lm,e} = \frac{(T_{17} - T_{10}) - (T_{18} - T_9)}{\ln \frac{(T_{15} - T_8)}{(T_{16} - T_8)}} \quad (7)$$

### Condenser

In the Condenser, a heat exchange occurs between the refrigerant fluid and the condensation water that is coming from the external source, Equations (8) e (9). Thus, heat is released by the ARS and the superheated water vapor is converted into saturated liquid water. Therefore, the energy balance in the Condenser is given by Equation (10).

$$\dot{m}_7 = \dot{m}_8 \quad (8)$$

$$\dot{m}_{15} = \dot{m}_{16} \quad (9)$$

$$\dot{Q}_c = \dot{m}_8 h_8 - \dot{m}_7 h_7 \quad (10)$$

where  $\dot{m}_7$ ,  $\dot{m}_8$ ,  $h_7$ ,  $h_8$  are the mass and enthalpy flow of refrigerant fluid in the entrance and exit of the Condenser. On the other hands,  $\dot{m}_{15}$ ,  $\dot{m}_{16}$  are the mass flow in the entrance and exit of condensation water from the external source.

The heat transfer rate,  $\dot{Q}_c$ , occurs simultaneously between the Condenser and the external source, Equation (11). Consequently, the logarithmic mean temperature difference (LMTD) method is used according to Equation (12) to modulate this component.

$$\dot{Q}_c = UA_c \Delta T_{lm,c} \quad (11)$$

$$\Delta T_{lm,c} = \frac{(T_{15} - T_8) - (T_{16} - T_8)}{\ln \frac{(T_{15} - T_8)}{(T_{16} - T_8)}} \quad (12)$$

### Absorber

In the Absorber, a heat exchange occurs between the refrigerant fluid and the condensation water that is coming from the external source, Equation (13) and Equation (15). Thus, heat is released by the ARS and the weak solution of water vapor is absorbed by a strong solution of water-lithium bromide which flows back to the Absorber. The Equation (14) represents the product of mass flow versus strong,  $x_1$  and weak,  $x_6$ ,

concentration of lithium bromide solution. The energy balance in the Absorber is given by Equation (16).

$$\dot{m}_1 = \dot{m}_6 + \dot{m}_{10} \quad (13)$$

$$\dot{m}_1 x_1 = \dot{m}_6 x_6 \quad (14)$$

$$\dot{m}_{13} = \dot{m}_{14} \quad (15)$$

$$\dot{Q}_a = \dot{m}_{10} h_{10} + \dot{m}_6 h_6 - \dot{m}_1 h_1 \quad (16)$$

where  $\dot{m}_6, \dot{m}_{10}, h_6, h_{10}$  are the mass and enthalpy flow of refrigerant fluid in the entrance of the Absorber. While  $\dot{m}_1, h_1$  are the mass and enthalpy flow of refrigerant fluid in the exit of the Absorber,  $\dot{m}_{13}, \dot{m}_{14}$  are the mass flow in the entrance and exit of condensation water from the external source.

The heat transfer rate,  $\dot{Q}_a$ , given by Equation (17), occurs simultaneously between the Absorber and the external source. Consequently, the logarithmic mean temperature difference (LMTD) method is used according to Equation (18) to modulate this component.

$$\dot{Q}_a = UA_a \Delta T_{lm,a} \quad (17)$$

$$\Delta T_{lm,a} = \frac{(T_6 - T_{14}) - (T_1 - T_{13})}{\ln \frac{(T_6 - T_{14})}{(T_1 - T_{13})}} \quad (18)$$

### Thermal Generator

In the Thermal Generator, a heat exchange occurs between the refrigerant fluid and the hot water that is coming from the Solar Collector, Equation (19) and Equation (20). Thus, heat is absorbed by the ARS and it occurs the vaporization of water present in the lithium bromide solution. Assuming the vapor that leaves the Thermal Generator is free of salt, the Equation (21) represents the product of mass flow versus concentration,  $x_3$  and  $x_4$ , of lithium bromide solution. Therefore, the energy balance in the Thermal Generator is given by Equation (22).

$$\dot{m}_3 = \dot{m}_4 + \dot{m}_7 \quad (19)$$

$$\dot{m}_{11} = \dot{m}_{12} \quad (20)$$

$$\dot{m}_3 x_3 = \dot{m}_4 x_4 \quad (21)$$

$$\dot{Q}_g = \dot{m}_4 h_4 + \dot{m}_7 h_7 - \dot{m}_3 h_3 \quad (22)$$

where  $\dot{m}_4, \dot{m}_7, \dot{m}_3, h_4, h_7, h_3$  are the mass and enthalpy flow of refrigerant fluid in the entrance and exit of the Thermal Generator. On other hands,  $\dot{m}_{11}, \dot{m}_{12}$  are the mass flow in the entrance and exit of hot water from the Solar Collector.

The heat transfer rate,  $\dot{Q}_g$ , given by Equation (23), occurs simultaneously between the Thermal Generator and the Solar Collector. Consequently, the logarithmic mean temperature difference (LMTD) method is used according to Equation (24) to modulate this component.

$$\dot{Q}_g = UA_g \Delta T_{lm,g} \quad (23)$$

$$\Delta T_{lm,g} = \frac{(T_{11} - T_4) - (T_{12} - T_7)}{\ln \frac{(T_{11} - T_4)}{(T_{12} - T_7)}} \quad (24)$$

### Heat Exchanger

In the Heat Exchanger, a heat exchange occurs between the strong LiBr solution that is returning from the Thermal Generator and the subcooled liquid solution that is flowing to the Thermal Generator. Thus, heat is absorbed by the ARS and the mixture of liquid and water vapor are converted into saturated water vapor. Therefore, the energy balance in the Heat Exchanger is between a cold,  $\dot{Q}_{tc}$  and hot,  $\dot{Q}_{tcq}$ , side that is given by Equation (25) and Equation (26).

$$\dot{Q}_{tcq} = \dot{m}_4 h_4 + \dot{m}_5 h_5 \quad (25)$$

$$\dot{Q}_{tc} = \dot{m}_3 h_3 - \dot{m}_2 h_2 \quad (26)$$

where  $\dot{m}_4, \dot{m}_5, h_4, h_5$  are the mass and enthalpy flow of refrigerant fluid in exit of the Thermal Generator and  $\dot{m}_3, \dot{m}_2, h_3, h_2$  are the mass and enthalpy flow of refrigerant fluid in the entrance of the Thermal Generator. Admittedly in this case, mass flow is constant for each side of Heat Exchanger. Thus, the effectiveness of this Heat Exchanger is given by Equation (27).

$$\varepsilon_{tc} = \frac{T_4 - T_5}{T_4 - T_2} \quad (27)$$

Herold (2016) affirms the logarithmic mean temperature difference (LMTD) method is used according to Equation (29) to modulate this component.

$$\dot{Q}_{tc} = UA_{tc} \Delta T_{lm,tc} \quad (28)$$

$$\Delta T_{lm,tc} = \frac{(T_4 - T_3) - (T_5 - T_2)}{\ln \frac{(T_4 - T_3)}{(T_5 - T_2)}} \quad (29)$$

### Pump and Expansion Valve

In this ARS, while pump increases the pressure level, expansion valve decreases. Thus, both components are considered as ideal and the process as isentropic. Therefore, the temperature remains constant and the energy balance in the Pump is given by Equation (30).

$$\dot{W}_b = \dot{m}_2 h_2 - \dot{m}_1 h_1 \quad (30)$$

### Solar Collector

Moreira (2019) affirms that is possible to quantify a useful thermal energy of input,  $E_{cs}$ , in the system absorbed by the Solar Collector through the Equation (31).

$$E_{cs} = \frac{V \cdot C_p \cdot (T_4 - T_{19})}{3600} \quad (31)$$

where  $V$ ,  $C_p$  are the water volume to be heated and the specific heat of water, respectively. On the other hands,  $T_4$ ,  $T_{19}$  are the temperature of the hot water required by the Thermal Generator and the average temperature of Brasilia (Cresesb, 2017).

Alternatively, the area of Solar Collectors,  $A_{cs}$ , can be obtained through Equation (32) proposed by Ghodeshwar (2018).

$$A_{cs} = \frac{\dot{Q}_g}{KI} \quad (32)$$

where  $\dot{Q}_g$ ,  $K$ ,  $I$  are the heat transfer rate in the Thermal Generator, the efficiency of the Solar Collector and the average of solar normal irradiancies in Brasilia, respectively.

### Coefficient of Performance

The coefficient of performance, COP, is determined by the ratio between the desired effect over the energy supply and can be obtained through the Equation (33).

$$COP = \frac{\dot{Q}_e}{\dot{Q}_{gv}} \quad (33)$$

## RESULTS AND DISCUSSION

A set of operating conditions for a single-effect water/lithium bromide cycle with Heat Exchangers in Table 1 was based on (Herold, 2016) and generated by imposing mass and energy balances on the components as listed in mathematical equations.

The hardware schematic in Table 2 provides additional details on some of the key assumptions used in modeling this cycle. The pump work is negligible in this case because it is quite small as compared with the heat transfer rates associated with the other components. The total of fourteen input parameters was varied to obtain successful results found by (Herold, 2016). Besides, the author varied each input parameter nine times to obtain the thermodynamic behaviors. It should be noted that each input parameter has different increment according to their own units.

Table 1. Set of Operating Conditions (Herold, 2016).

State Points	h (kJ/kg)	$\dot{m}$ (kg/s)	P (kPa)	Vapor Quality	T (°C)	x (% LiBr)
1	85.8	0.05	0.68	0	32.9	56.7
2	85.8	0.05	7.353		32.9	56.7
3	147	0.05	7.353		63.2	56.7
4	221.2	0.0455	7.353	0	89.4	62.4
5	153.9	0.0455	7.353		53.2	62.4
6	153.9	0.0455	0.68	0.006	44.7	62.4
7	2643.3	0.0455	7.353		76.8	0
8	167.2	0.0455	7.353	0	39.9	0
9	167.2	0.0455	0.68	0.064	1.5	0
10	2503.2	0.0455	0.68	1	1.5	0
11	419.1	1			100	
12	404.4				96.5	
13	104.8	0.28			25	
14	154.9				37	
15	104.8	0.28			25	
16	144.8				34.6	
17	42	0.4			10	
18	15.6				3.7	

Table 2. Hardware Schematic.

Baseline Inputs Defining Single-Effect Operating Conditions in Table 1		Variation of Input Parameters for Parametric Analyses			Baseline Outputs Defining Single-Effect Operating Conditions in Table 1	
Input Parameter	Value	First Value	Increment	Final Value	Output Parameter	Value
$\varepsilon_{tc}$	0.64	0.56	0.02	0.72	$\Delta T_{m,c}$ (K)	9.34
$\dot{m}_1$ (kg/s)	0.05	0.03	0.005	0.07	$\Delta T_{m,g}$ (K)	14.674
$UA_a$ (kW/K)	1.8	1.4	0.1	2.2	$\Delta T_{m,a}$ (K)	7.8
$UA_c$ (kW/K)	1.2	0.8	0.1	1.6	$\Delta T_{m,e}$ (K)	4.7
$UA_g$ (kW/K)	1	0.6	0.1	1.4	$\Delta T_{m,tc}$ (K)	23.15
$UA_e$ (kW/K)	2.25	1.85	0.1	2.65	$\dot{Q}_a$ (kW)	14.04
$T_{13}$ (°C)	25	21	1	29	$\dot{Q}_e$ (kW)	10.575
$\dot{m}_{13}$ (kg/s)	0.28	0.26	0.005	0.3	$\dot{Q}_{tc}$ (kW)	3.062
$T_{15}$ (°C)	25	21	1	29	$\dot{Q}_c$ (kW)	11.209
$\dot{m}_{15}$ (kg/s)	0.28	0.26	0.005	0.3	$\dot{Q}_g$ (kW)	14.67
$T_{11}$ (°C)	100	96	1	104	COP	0.721
$\dot{m}_{11}$ (kg/s)	1	0.98	0.005	1.02	$\dot{W}_b$ (kW)	0.206
$T_{17}$ (°C)	10	6	1	14		
$\dot{m}_{17}$ (kg/s)	0.4	0.38	0.005	0.42		

After adding increments of 0.005 °C for nine times, it was possible to verify the influence of  $\dot{m}_1$ . Then, the increases of  $\dot{Q}_g$ ,  $\dot{Q}_a$  and decreases of COP are noted in Figure 3. It happens because the heat flow that is absorbed by the Thermal Generator increases, while the heat flow absorbed by the Evaporator does not have significant changes.

After adding increments of 0,1 kW/K for nine times, it was possible to verify the same influence of all thermal conductance's  $UA_a$ ,  $UA_c$ ,  $UA_g$  and  $UA_e$ . It happens because by increasing the material's ability to conduct heat, the logarithmic mean temperature difference between the fluids from external sources and the H<sub>2</sub>O-LiBr fluid is raised.



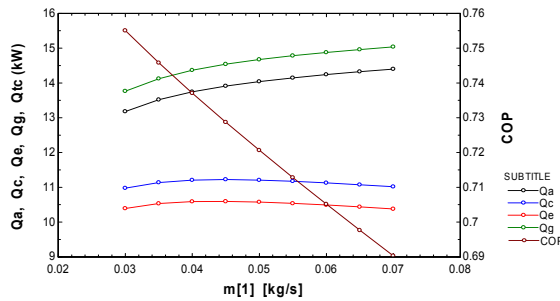


Figure 3. Behavior of entrance mass flow parameter.

Then, the increases of  $\dot{Q}_e$ ,  $\dot{Q}_g$ ,  $\dot{Q}_a$ ,  $\dot{Q}_c$  and the low reduction of COP are noted in Figure 4 represented by  $UA_g$  parameter.

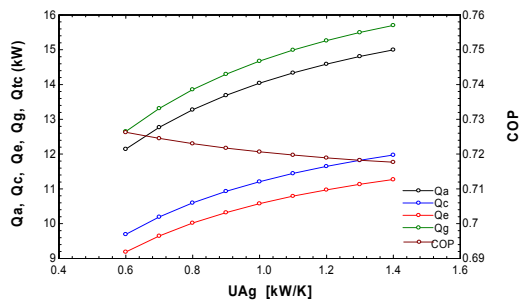


Figure 4. Behavior of Thermal Generator UA parameter.

After adding increments of 1°C for nine times, it was possible to verify the influence of  $T_{17}$ . Then, the increases of  $\dot{Q}_e$ ,  $\dot{Q}_g$ ,  $\dot{Q}_a$ ,  $\dot{Q}_c$  and COP are noted in Figure 5. It happens because the evaporation temperature and the heat flow absorbed in the Evaporator are increased when the temperature of cold water is raised. As a result, it will have more saturated water vapor being absorbed by the LiBr solution and more heat being absorbed in the Thermal Generator.

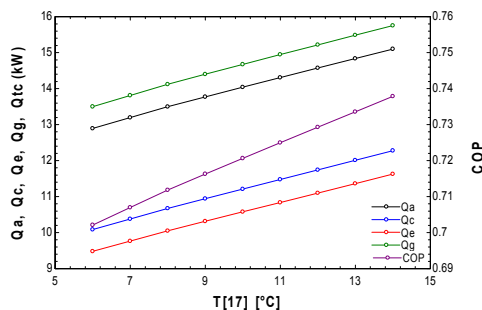


Figure 5. Behavior of cold water temperature parameter.

Heat exchangers with indirect contact as used in the system do not mix fluids from external sources with the  $H_2O$ -LiBr fluid. Therefore, there were not significant increases in the mass flow of refrigerant

vapor caused by external sources  $\dot{m}_{13}$ ,  $\dot{m}_{15}$ ,  $\dot{m}_{11}$ ,  $\dot{m}_{17}$ . It was undoubtedly necessary to verify the influence of  $T_{11}$  after adding increments of 1°C for nine times

Then, the increases of  $\dot{Q}_e$ ,  $\dot{Q}_g$ ,  $\dot{Q}_a$ ,  $\dot{Q}_c$  and the low variation of COP are noted in Figure 6. It happens because when the temperature of Thermal Generator hot water is raised, it will have as a result a solution more concentrated returning to the Absorber and more quantity of steam flowing to the Condenser.

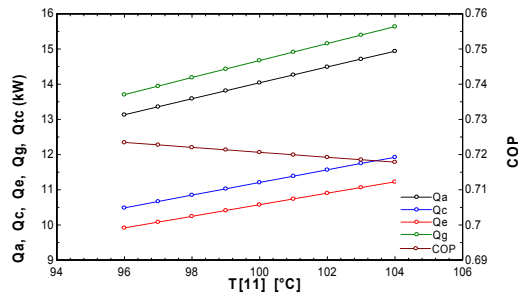


Figure 6. Behavior of Thermal Generator hot water temperature parameter.

After adding increments of 1°C for nine times, it was possible to verify the same influence of condensation water temperature  $T_{13}$  and  $T_{15}$  over the decreasing of  $\dot{Q}_e$ ,  $\dot{Q}_g$ ,  $\dot{Q}_a$ ,  $\dot{Q}_c$  and COP. It happens because the lower condensation water temperature  $T_{13}$ , the greater the water vapor absorption capacity from the Evaporator. On the other hands, as the condensation water leaves the Absorber at a higher temperature, the heat transfer capacity in the Condenser is reduced. The behavior of these results can be visualized graphically by Fig. 7 and 8.

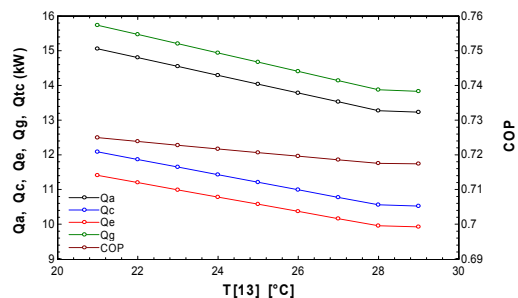


Figure 7. Behavior of Absorber condensation water temperature parameter.

The parametric analysis of hot water temperature  $T_4$  required by the Thermal Generator is an adaptation to the cycle proposed by Herold (2016). Therefore, it is the last parameter to be analyzed and varied between 80 to 94 °C in increments of 2°C. There was an increase in the useful energy,  $E_{cs}$ , absorbed by the Solar Collector and also an increase in the area,  $A_{cs}$ , of Solar Collectors required as shown in Fig. 9.



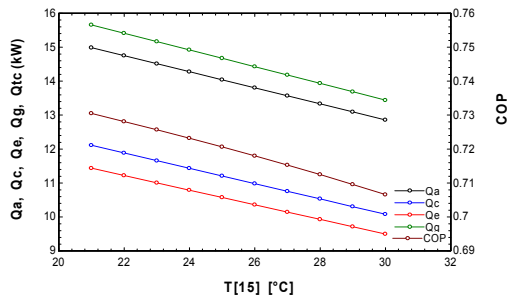


Figure 8. Behavior of Condenser condensation water temperature parameter.

It happens because the higher the water temperature required by the Thermal Generator, the greater the number of Solar Collectors to absorb the necessary thermal energy that will be used to supply the refrigeration cycle.

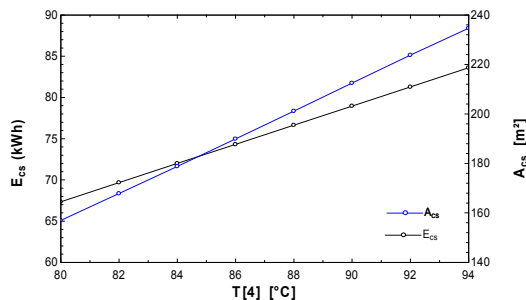


Figure 9. Behavior of hot water temperature required by the Thermal Generator.

## CONCLUSIONS

After all results considered, there are no doubts about notable variations of input parameters over output parameters. However, the most relevant were: mass flow of the H<sub>2</sub>O-LiBr solution and the temperature of cold water, T<sub>17</sub>. Besides, it was possible to conclude that the temperatures from external sources should be considered one of the most sensitive parameters to the absorption refrigeration system especially because it was showed different behaviors in the heat transfer rate and in the COP.

The data's introduced in the Solar Collector area and the useful energy can be used in future works to determine the quantity of Solar Collectors necessary to supply the system, the economic viability and the time lag between investment and payback. Another suggestion would be to analyze the viscosity as an input parameter since it also depends on the system temperature but was not included in this work.

Although, the general objectives were successfully attended and clearly the parametric analyses allowed to verify, validate and perform the single-effect absorption refrigeration system proposed by Herold (2016). In conclusion, the sensitivity of the values found demonstrate the crucial importance of accomplish a

parametric analysis to optimize thermal engineering projects.

## REFERENCES

- Costa, E. C. Refrigeração. São Paulo. 3ª Edição. Editora Edgard Blucher Ltda, 1985.
- CRESESB, SunData. Centro de Referência para Energia Solar e Eólica Sérgio Brito / CEPEL Potencial Solar. <http://www.cresesb.cepel.br/index.php#data>; 2017 (acessado 10 de Outubro 2020).
- Ghodeswar, A. Thermodynamic Analysis of Lithium Bromide-Water (LiBr-H<sub>2</sub>O) Vapor Absorption Refrigeration System Based on Solar Energy. v.5, p.1365-1371, 2018.
- Herold, K. E. Absorption Chillers and Heat Pump, 2ª Edição, Editora CRC Press, 2016.
- Moreira, S. Energias Renováveis, Geração Distribuída e Eficiência Energética. 1ª Edição. Editora LTC, 2019.
- Pereira, E. B. Atlas Brasileiro de Energia Solar. INPE, 2ª Edição. São José dos Campos, 2017.
- Reis, L. B. Energia, recursos naturais e a prática do desenvolvimento sustentável. 3ª Edição. Editora Manole Ltda, 2019.
- Sonda INPE - Sistema de Organização Nacional de Dados Ambientais; <http://sonda.ccst.inpe.br/>; 2020 (acessado 13 de Outubro 2020).